HOXB13 suppresses proliferation, migration and invasion, and promotes apoptosis of gastric cancer cells through transcriptional activation of VGLL4 to inhibit the involvement of TEAD4 in the Hippo signaling pathway

HUI GENG, GUANGLI LIU, JIANDONG HU, JIANCHAO LI, DONG WANG, SHENSHAN ZOU and XINTAO XU

Department of General Surgery, Changzhou Hospital of Traditional Chinese Medicine, Changzhou, Jiangsu 213003, P.R. China

Abstract. Gastric cancer (GC) is one of the most common types of malignancy worldwide and is accompanied by both high mortality and morbidity rates. Homeobox B13 (HOXB13) has been reported to act as a tumor suppressor gene in multiple types of human cancer. The present study aimed to investigate the effects and potential underlying molecular mechanisms of HOXB13 in the progression of GC. The expression of HOXB13 in GC cells was first examined using the Cancer Cell Line Encyclopedia database and subsequently validated in a number of GC cell lines. Following HOXB13 overexpression (Ov-HOXB13), HGC-27 cell proliferation was evaluated by colony formation and Cell Counting Kit-8 assays. Wound healing and Matrigel assays were used to determine the migratory and invasive abilities, respectively. Additionally, cell apoptosis was assessed using TUNEL staining, and the expression of apoptosis-related proteins was detected by western blot analysis. Subsequently, TEA domain transcription factor 4 (TEAD4) was overexpressed to evaluate the effects on HGC-27 cell proliferation, migration, invasion and apoptosis following co-transfection with Ov-HOXB13. The potential binding sites of HOXB13 on the vestigial-like family member 4 (VGLL4) promoter were verified using chromatin immunoprecipitation and dual luciferase reporter assays. Moreover, the expression levels of proteins involved in the Hippo signaling pathway were analyzed using western blotting. The results revealed that the expression of HOXB13 was notably lower in GC cells compared with normal gastric cells. The overexpression of HOXB13 significantly inhibited the proliferation, migration and invasion, but promoted the apoptosis of HGC-27 cells. Moreover, Ov-HOXB13 downregulated TEAD4 expression. Notably, Ov-TEAD4 transfection partially reversed the effects of Ov-HOXB13 on the cellular behaviors of HGC-27 cells. HOXB13 was also confirmed to bind with the VGLL4 promoter. The knockdown of VGLL4 restored the inhibitory effects of Ov-HOXB13 on the expression levels of VGLL4 and Hippo pathway signaling proteins. In conclusion, the findings of the present study suggested that Ov-HOXB13 may suppress the proliferation, migration and invasion, and promote the apoptosis of GC cells through the transcriptional activation of VGLL4 to inhibit the involvement of TEAD4 in the Hippo signaling pathway. These results may provide novel and potent targets for the treatment of GC.

Introduction

Gastric cancer (GC) is the third most common cause of cancer-related mortality worldwide. After surgical removal of cancer tissue, the five-year survival rate of patients with stage II GC is still <35% (1). Previous studies have shown that risk factors for GC include chronic infection of *Helicobacter pylori*, age, radiation exposure, low socioeconomic status and low levels of physical activity (2,3). The morbidity of GC progressively increases with age, with the median age at diagnosis being 70 years; however, at present, ~10% of GC cases are diagnosed at the age of 45 or younger (2). Thus, it is of great importance to determine the potential underlying mechanisms of GC progression.

Homeobox B13 (HOXB13) is an important member of the HOX family, which encode nuclear transcription factors that drive cell differentiation during normal development and tumorigenesis (4). HOXB13 has been reported to act as a tumor suppressor gene in a number of types of human cancer, including colon cancer (5), prostate cancer (6) and renal cell carcinoma (7). A previous study demonstrated that HOXB13 expression was significantly downregulated in primary GC tissues compared with the corresponding non-malignant gastric tissues, and HOXB13 expression was positively correlated with the 5-year overall survival rate (8). This finding suggested that HOXB13 may also act as a tumor suppressor gene in GC progression and may have potential as a promising

Correspondence to: Dr Xintao Xu, Department of General Surgery, Changzhou Hospital of Traditional Chinese Medicine, 25 Heping North Road, Tianning, Changzhou, Jiangsu 213003, P.R. China
E-mail: xintaoxu23@163.com

biomarker for the diagnosis and prognosis of GC. Although studies have shown that the mechanism of HOXB13 in GC may be related to its own methylation and regulation of the IGF-1R/PI3K/AKT/mTOR pathway (8,9), the specific underlying mechanism of the effects of HOXB13 in GC remains to be further elucidated. Thus, the present study aimed to investigate the potential underlying mechanism of HOXB13 in GC progression.

TEA domain (TEAD)1 and TEAD4 are key effectors of the Hippo signaling pathway and have been reported to exert oncogenic roles in gastric tumorigenesis (10). Notably, the Hippo signaling pathway was previously found to serve a regulatory role in GC tumorigenesis (11). Vestigial-like family member 4 (VGLL4) was discovered to act as a tumor suppressor in GC by directly competing with Yes1-associated transcriptional regulator (YAP) to bind to TEADs, thereby suppressing the tumor-promoting effect of the TEAD family in GC (12). Hence, the present study explored whether the HOXB13-mediated regulation of GC cell progression was related to TEAD4 and VGLL4.

The present study aimed to determine the effects of HOXB13 on the proliferation, migration, invasion and apoptosis of GC cells and to investigate the underlying mechanism to provide a novel insight into the current understanding of the pathogenesis of GC.

Materials and methods

Bioinformatics Methods. The interaction between HOXB13 and TEAD4 was predicted using the Search Tool for the Retrieval of Interacting Genes/Proteins (STRING) database (https://string-db.org/cgi/input.pl). HOXB13 was identified as a transcription factor of VGLL4 using the JASPAR database (http://jaspar.genereg.net).

Cell lines and culture. Human GC cell lines, including MKN-45, MKN-74, AGS and HGC-27, and normal gastric GES-1 cells were obtained from the American Type Culture Collection. Cells were cultured in DMEM/F12 1:1 medium (HyClone; Cytiva) supplemented with 10% FBS (HyClone; Cytiva) and maintained at 37°C with 5% CO_2.

Cell transfection. HOXB13 expression in GC cell lines was examined using the Cancer Cell Line Encyclopedia (CCLE; https://portals.broadinstitute.org/ccle). HOXB13 overexpression (Ov-HOXB13), TEAD4 overexpression (Ov-TEAD4) and pcDNA3.1 negative control (Ov-NC) plasmids were purchased from Shanghai GenePharma Co., Ltd. Briefly, $2x10^4$ HGC-27 cells/well were transfected with 100 pmol pcDNA3.1 vectors using Lipofectamine® 2000 (Invitrogen; Thermo Fisher Scientific, Inc.) according to the manufacturer's protocol. Subsequently, cells were transfected with either small interfering RNA (siRNA) targeting VGLL4 (si-VGLL4-1, 5'-AGGACCTAGACTGTGACAA-3'; si-VGLL4-2, 5'-TCGCACTGACCAAGAACAG-3') or si-NC (5'-CUAGAACUGGACAACGACA-3') according to the manufacturer's protocol. All the siRNAs were used at a final concentration of 10 nM. After transfection at 37°C for 6 h, the medium was replaced with complete medium. Then, following incubation at 37°C for 36 h, the transfection efficiencies

of the overexpression plasmids and siRNAs were verified using reverse transcription-quantitative PCR (RT-qPCR) and western blotting, and the most effective siRNA was used for the subsequent functional experiments.

Cell viability assay. Viability of HGC-27 cells was determined using a Cell Counting Kit-8 (CCK-8) assay (Beyotime Institute of Biotechnology). Briefly, $2x10^3$ cells/well were seeded into 96-well plates and cultured at 37°C for 24 h. After the indicated transfections, 10 μl CCK-8 reagent was added to each well and incubated at 37°C for an additional 4 h. The absorbance was measured at a wavelength of 450 nm using an automated microplate reader (Beckman DU6400 spectrophotometer; Beckman Coulter, Inc.).

Colony formation assay. Following transfection, mixed $1x10^3$ HGC-27 cells with 1 ml 0.3% soft agar and inoculated them into 6-well plates pre-plated with 1.5 ml 0.6% soft agar and cultured at 37°C for 2 weeks with complete medium in a 5% CO_2 incubator. After colony formation, colonies were fixed with 4% paraformaldehyde (Biosharp Life Sciences) for 20 min and stained with 1% crystal violet (Nanjing Biotech Co., Ltd.) for 30 min at room temperature. Colonies were counted using an inverted light microscope (Olympus Corporation).

Wound healing assay. HGC-27 were seeded ($1x10^5$ cells/well) into 6-well plates and cultured at 37°C overnight. After reaching 80-90% confluence, the cells were transiently transfected for 6 h, and then cultured in complete medium at 37°C for an additional 18 h. An artificial wound was made by scratching the cell monolayer with a sterile pipette tip. Cells were washed with phosphate buffer solution (PBS) to remove the debris, and the media was replaced with serum-free DMEM/F12 1:1 medium. The plates and the wound closure were visualized at 0 and 24 h using an inverted light microscope (magnification, x100; Olympus Corporation). The ratio of the wound area to the initial wound area was calculated using ImageJ 1.46r (National Institutes of Health).

Transwell assay. The Transwell membranes were precoated with Matrigel, and the substrate membrane was air-dried at room temperature for 3 h and then hydrated with DMEM. Following transfection, $4x10^4$ HGC-27 cells/well were seeded into the upper chambers, in serum-free medium. A total of 500 μl complete medium supplemented with 10% FBS was added into the lower chambers as a chemoattractant. Following 24 h of incubation at 37°C, the cells were fixed with 4% paraformaldehyde for 10 min and stained with 1% crystal violet for 20 min at room temperature. The invading cells were counted using an inverted light microscope (Olympus Corporation; magnification, x200) in five pre-determined fields of view.

TUNEL staining. Following transfection, HGC-27 cells ($2x10^6$ cells/well in 6-well plates) were fixed with 4% paraformaldehyde at room temperature for 30 min, washed with PBS and incubated with 0.3% Triton-X 100 for 5 min to permeabilize the cell membrane. Apoptosis was analyzed using a TUNEL Apoptosis Detection kit (Beyotime Institute of Biotechnology) according to the manufacturer's protocol. Briefly, cells were incubated with 50 μl TUNEL reaction buffer

for 1 h at 37°C in the dark. The nuclei were counterstained with DAPI for 5 min at room temperature in the dark and the slides were then mounted with anti-fade mounting medium. The levels of apoptosis were estimated as the ratio of the number of TUNEL-positive cells to the total number of DAPI-positive cells using a fluorescence microscope (magnification, x200; Olympus Corporation).

Dual luciferase reporter gene assay. Luciferase reporter plasmids (Promega Corporation) were constructed with wild-type (WT) and mutant-type (MUT) 3'-untranslated region sequences. The MUT sequences included MUT-VGLL4-SITE1 (S1; -1,061 to -1,052) and MUT-VGLL4-SITE2 (S2; -1,876 to -1,867). Firefly luciferase was used as the primary reporter to monitor the binding of the protein to the cloned target sequences. *Renilla* luciferase was used as the control reporter for normalization. The luciferase reporter plasmids and regulating factors were co-transfected into HGC-27 cells using Lipofectamine® 3000 reagent (Invitrogen; Thermo Fisher Scientific, Inc.). All plasmids were used at a concentration of 50 ng per well in the 12-well plates. After transfection at 37°C for 6 h, fresh complete medium was replaced, and luciferase activities of different groups were detected until 48 h after transfection. The relative luciferase activities were measuring using a Dual Luciferase Reporter assay system (Promega Corporation).

Chromatin immunoprecipitation (ChIP) assay. The binding of HOXB13 to the VGLL4 promoter was validated using a ChIP assay kit (Beyotime Institute of Biotechnology) according to the manufacturer's protocol. Briefly, formaldehyde was added at a final concentration of 1% to the cultured HGC-27 cells and incubated at room temperature for 10 min to cross-link the protein and DNA; then three sets of 20-sec pulses were used to obtain chromatin fragments. An anti-HOXB13 antibody (1:20; cat. no. ab201682; Abcam) was used to generate the immunoprecipitations and an anti-IgG antibody (1:40; cat. no. sc-2025; Santa Cruz Biotechnology, Inc.) was used as the blank control group to exclude the influence of other factors in the ChIP assay. The recovered DNA fragments were evaluated using RT-qPCR. The primer sequences were as follows: VGLL4, forward 5'-AACTGCAACCTCTCGCACTG-3' and reverse 5'-GCTCGGGCTCCTTGTAATTCT-3'.

RT-qPCR. Total RNA was extracted from $1x10^5$ cells using TRIzol® reagent (Thermo Fisher Scientific, Inc.) according to the manufacturer's instructions. Total RNA was reverse transcribed into cDNA using PrimeScript™ RT reagent Kit (Takara Bio, Inc.). qPCR was subsequently performed in a 96-well optical plate using Thunderbird SYBR qPCR mix (Toyobo Life Science) and an ABI Prism 7500 Real-Time PCR Detection System (Applied Biosystems; Thermo Fisher Scientific, Inc.). The following thermocycling conditions were used for the qPCR: Initial denaturation at 95°C for 1 min, followed by 40 cycles of 95°C for 15 sec and 60°C for 1 min. The relative expression levels of HOXB13, TEAD4 and VGLL4 were calculated using the $2^{-\Delta\Delta Cq}$ method (13) and normalized to GAPDH. The primer sequences were as follows: VGLL4, forward 5'-GGCAGCATTTGCAGACTCCAG-3' and reverse 5'-GGTGATGAACTTGTTAGCCGC-3'; TEAD4,

forward 5'-CTGGACAAGCCCATCGACAA-3' and reverse 5'-CAGCTCGTTCCGACCATACA-3'; and VGLL4, forward 5'-TTTGTGAAGTTGAAGAGCCAGG-3' and reverse 5'-GCAGCTTCGCCTTCGT-3'. All experiments were performed in triplicate.

Western blotting. Total protein was extracted from cells ($2x10^6$) using RIPA lysis buffer (Beyotime Institute of Biotechnology). Total protein concentration was determined using the BCA method and 20 μg protein/lane was separated by 10% SDS-PAGE. The separated proteins were transferred onto PVDF membranes and blocked with 5% skimmed milk for 2 h at room temperature. The membranes were then incubated with following primary antibodies overnight at 4°C: Anti-HOXB13 (1:1,000; cat. no. ab201682; Abcam), anti-proliferating cell nuclear antigen (PCNA; 1:1,000; cat. no. ab92552; Abcam), anti-Ki-67 (1:1,000; cat. no. ab92742; Abcam), anti-MMP2 (1:1,000; cat. no. ab92536; Abcam), anti-MMP9 (1:1,000; cat. no. ab76003; Abcam), anti-issue inhibitor of metalloproteinases 1 (TIMP-1; 1:1,000; cat. no. ab211926; Abcam), anti-Bcl-2 (1:1,000; cat. no. ab182858; Abcam), anti-Bax (1:1,000; cat. no. ab32503; Abcam), anti-cleaved caspase-3 (1:500; cat. no. ab32042; Abcam), anti-caspase-3 (1:1,000; cat. no. ab32351; Abcam), anti-TEAD4 (1:1,000; cat. no. ab155244; Abcam), anti-cellular communication network factor 2 (CCN2; 1:1,000; cat. no. ab209780; Abcam), anti-cysteine rich angiogenic inducer 61 (Cyr61; 1:1,000; cat. no. ab230947; Abcam), anti-amphiregulin (AREG; 1:1,000; cat. no. ab180722; Abcam) and anti-GAPDH (1:2,000; cat. no. ab181602; Abcam). Following the primary antibody incubation, the membranes were washed three times with TBS +0.05% Tween-20 and incubated with a goat anti-rabbit HRP-conjugated secondary antibody (1:1,000; cat. no. ab6721; Abcam) at room temperature for 2 h. Protein bands were visualized using a Pierce ECL Plus Western Blotting (Pierce; Thermo Fisher Scientific, Inc.) and analyzed using ImageJ (version 1.8; National Institutes of Health).

Statistical analysis. All experiments were repeated three times. All data are reported as the mean ± standard deviation and analyzed with GraphPad Prism 8.0 software (GraphPad Software, Inc.). One-way ANOVA followed by Tukey's post-hoc test was used to compare differences among multiple groups. $P<0.05$ was considered to indicate a statistically significant difference.

Results

HOXB13 expression levels are notably lower in GC tissues and cell lines. Analysis of the CCLE database revealed that HOXB13 expression was lower in GC tissues compared with normal gastric tissues (Fig. 1A). Results from western blotting and RT-qPCR analyses demonstrated that HOXB13 protein and mRNA expression levels, respectively, were also significantly lower in MKN-45, MKN-74 and HGC-27 cells compared with GES-1 cells, while HOXB13 was only significantly reduced in AGS cells at the mRNA level, and the expression levels were lowest in HGC-27 cells (Fig. 1B and C). Therefore, the HGC-27 cell line was selected for use in subsequent experiments. These results suggested that HOXB13 may be involved in GC progression.
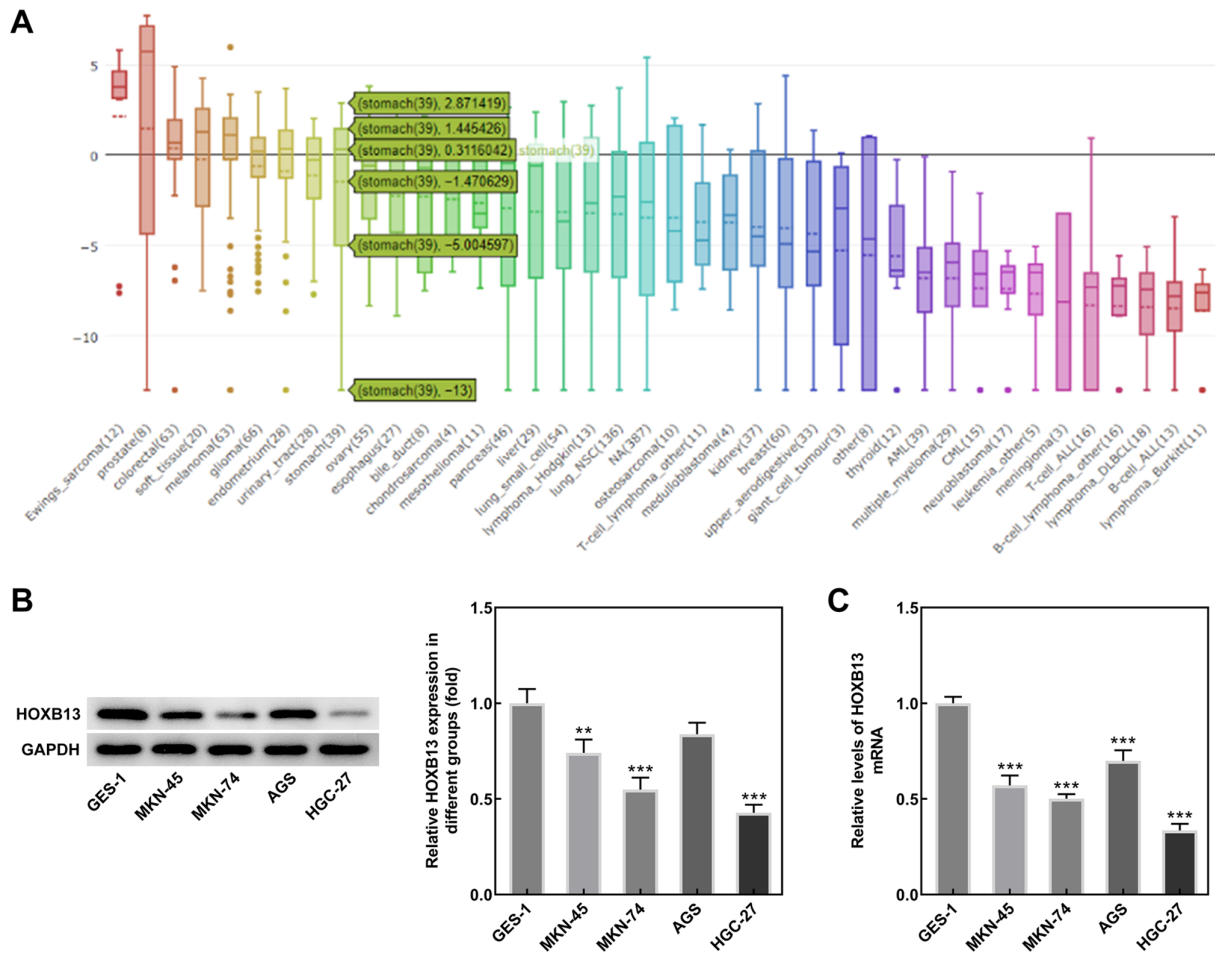
Figure 1. HOXB13 expression levels are significantly lower in GC cell lines. (A) HOXB13 expression was lower in GC tissues than normal gastric tissues, as determined by the analysis of the Cancer Cell Line Encyclopedia database. (B) Protein and (C) mRNA expression levels of HOXB13 in several human GC cell lines (MKN-45, MKN-74, AGS and HGC-27) and GES-1 normal gastric cells were detected using western blotting and reverse transcription-quantitative PCR, respectively. **P<0.01, ***P<0.001 vs. GES-1. GC, gastric cancer; HOXB13, homeobox B13.

Overexpression of HOXB13 inhibits the proliferation, migration and invasion of HGC-27 GC cells. To investigate the role of HOXB13 in the progression of GC, HGC-27 cells were successfully transfected with Ov-HOXB13 plasmid, as demonstrated by RT-qPCR (Fig. 2A). Ov-HOXB13 transfection notably inhibited the proliferative ability of HGC-27 cells compared with the Ov-NC group (Fig. 2B and C). Ov-HOXB13 also significantly downregulated the expression levels of the proliferation-related markers, PCNA and Ki-67, compared with the Ov-NC group (Fig. 2D). Moreover, the results from the wound healing and Transwell assays showed that the overexpression of HOXB13 significantly decreased the migratory and invasive abilities of HGC-27 cells (Fig. 2E and F, respectively), and downregulated the protein expression levels of the migration- and invasion-related proteins, TIMP-1, MMP2 and MMP9 (Fig. 2G). These results suggested that Ov-HOXB13 may inhibit the proliferation, migration and invasion of HGC-27 cells.

Overexpression of HOXB13 promotes the apoptosis of HGC-27 GC cells. To further investigate the effects of HOXB13 in GC progression, cell apoptosis was detected using a TUNEL assay following the overexpression of HOXB13 in HGC-27 cells. As shown in Fig. 3A and B, the cell apoptotic rate was notably

increased following the overexpression of HOXB13. In addition, the expression levels of the anti-apoptotic protein, Bcl-2, were downregulated following the overexpression of HOXB13, whereas the expression levels of the proapoptotic proteins, Bax and cleaved caspase-3, were upregulated following the overexpression of HOXB13 (Fig. 3C and D). These results indicated that Ov-HOXB13 may promote the apoptosis of HGC-27 cells.

Overexpression of HOXB13 downregulates TEAD4 expression in HGC-27 GC cells. To determine the mechanism underlying the role of HOXB13 in the development of GC, the interaction between HOXB13 and TEAD4 was predicted using the STRING database (Fig. 4A). Results from western blotting analysis and RT-qPCR revealed that the protein and mRNA expression levels of TEAD4 were higher in GC cell lines compared with GES-1 cells (Fig. 4B and C, respectively). Notably, Ov-HOXB13 transfection significantly downregulated the expression of TEAD4 (Fig. 4D and E), suggesting that the overexpression of HOXB13 may downregulate TEAD4 expression in HGC-27 cells.

Overexpression of TEAD4 reverses the effects of Ov-HOXB13 on the proliferation, migration, invasion and apoptosis of HGC-27 GC cells. To confirm whether TEAD4 mediated the
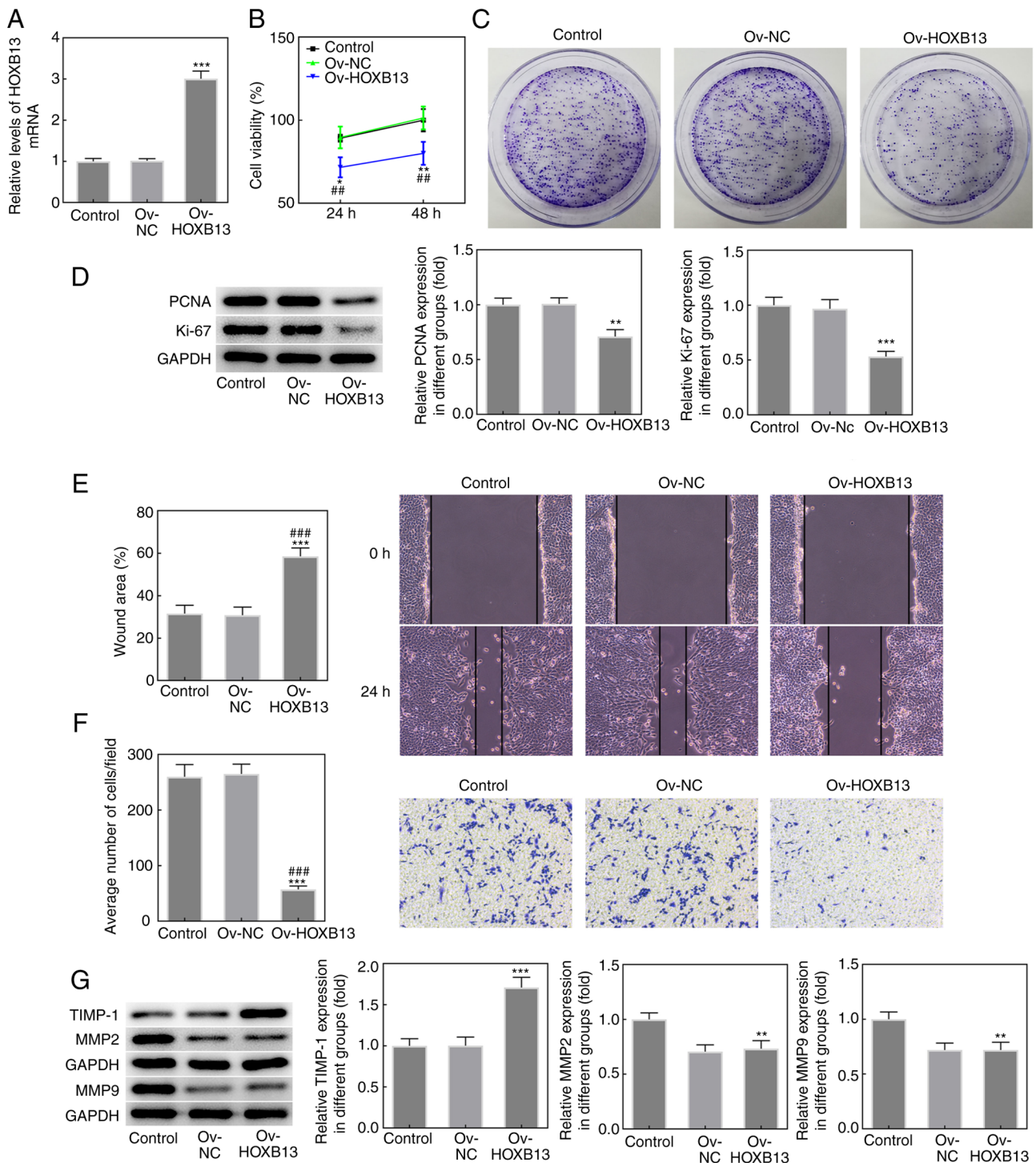
Figure 2. Overexpression of HOXB13 inhibits the proliferation, migration and invasion of HGC-27 gastric cancer cells. (A) Expression levels of HOXB13 in HGC-27 cells following transfection with Ov-HOXB13 plasmid were analyzed using reverse transcription-quantitative PCR. (B) Cell viability was detected using a Cell Counting Kit-8 assay. (C) Cell proliferation was analyzed using a colony formation assay. (D) Protein expression levels of PCNA and Ki-67 were determined by western blotting. (E) Cell migration was measured using a wound healing assay. (F) Cell invasion was analyzed using a Transwell assay. (G) Protein expression levels of TIMP-1, MMP2 and MMP9 were determined by western blotting. $^{*}P<0.05$, $^{**}P<0.01$, $^{***}P<0.001$ vs. Ov-NC; $^{##}P<0.01$, $^{###}P<0.001$ vs. Control. HOXB13, homeobox B13; NC, negative control; Ov, overexpression; PCNA, proliferating cell nuclear antigen; TIMP-1, tissue inhibitor of metalloproteinases 1.

effects of HOXB13 in GC progression, an Ov-TEAD4 plasmid was constructed, and the expression of TEAD4 was notably upregulated following transfection compared with the Ov-NC group (Fig. 5A). Additionally, as shown in Fig. 5B and C, the results from the western blotting and RT-qPCR analyses, respectively, demonstrated that co-transfection with the Ov-HOXB13

and Ov-TEAD4 plasmids upregulated TEAD4 expression levels in HGC-27 cells compared with co-transfection with the Ov-HOXB13 + Ov-NC plasmids group. In addition, the results of the CCK-8 and colony formation assays demonstrated that the overexpression of TEAD4 partially reversed the effects of the Ov-HOXB13 plasmid on the proliferation of HGC-27
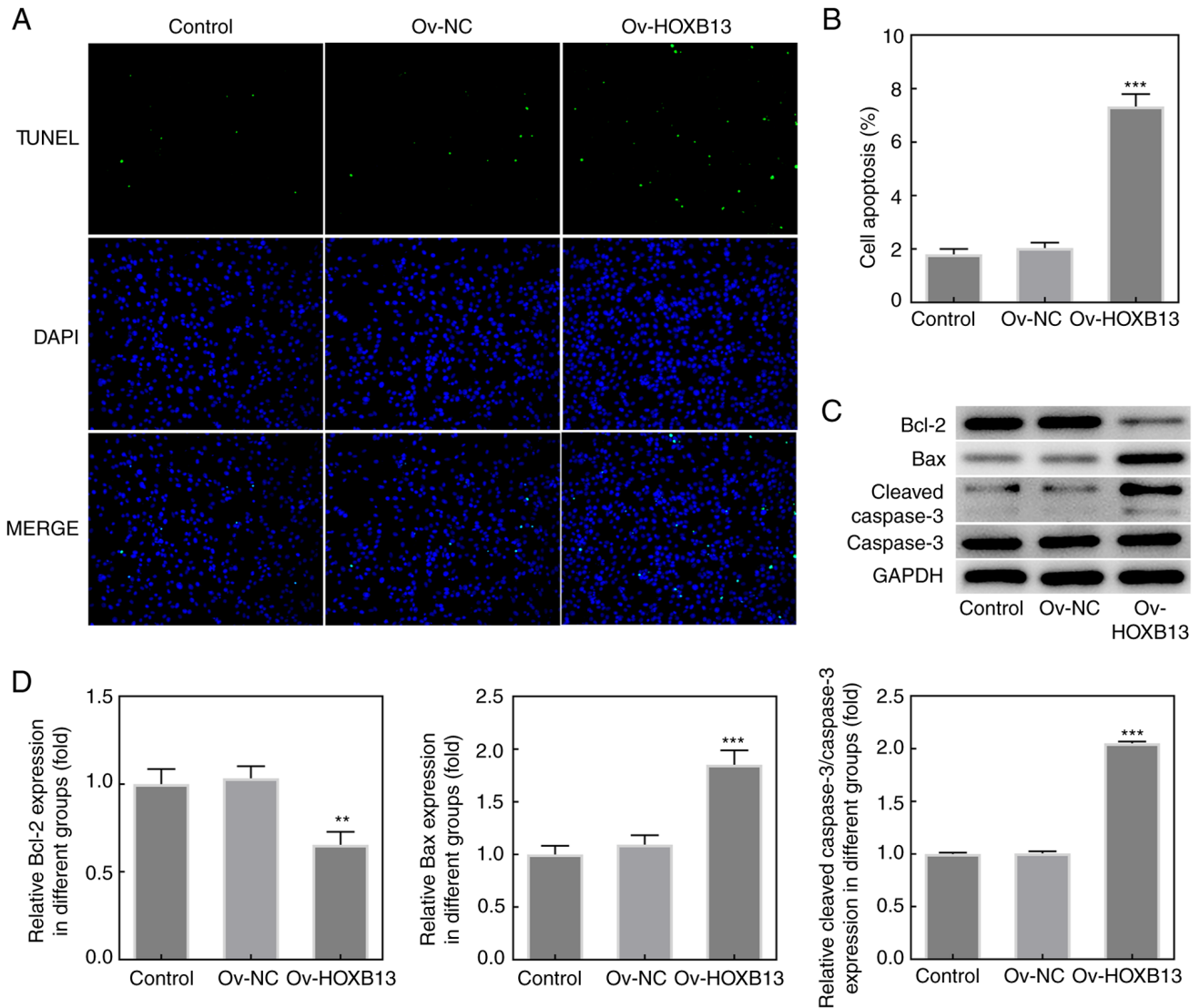
Figure 3. Overexpression of HOXB13 promotes the apoptosis of HGC-27 gastric cancer cells. (A) Cell apoptosis was evaluated using a TUNEL assay and (B) quantified. (C) Expression levels of apoptosis-related proteins, Bcl-2, Bax and cleaved caspase-3, were determined using western blotting and (D) semi-quantified. **P<0.01, ***P<0.001 vs. Ov-NC. HOXB13, homeobox B13; NC, negative control; Ov, overexpression.

cells (Fig. 5D and E, respectively). Similarly, the expression levels of PCNA and Ki-67 in HGC-27 cells co-transfected with Ov-HOXB13 and Ov-TEAD4 plasmids were markedly upregulated compared with the Ov-HOXB13 + Ov-NC group (Fig. 5F).

Moreover, the results from wound healing and Transwell assays demonstrated that the overexpression of TEAD4 blocked the suppressive effect of Ov-HOXB13 on the migration and invasion of HGC-27 cells (Fig. 6A and B, respectively), and the expression of TIMP-1, MMP2 and MMP9 (Fig. 6C). Notably, as shown in Fig. 7A and B, the apoptotic rate of HGC-27 cells co-transfected with Ov-HOXB13 and Ov-TEAD4 plasmids was decreased compared with the Ov-HOXB13 + Ov-NC group. Overexpression of TEAD4 reversed the effects of Ov-HOXB13 on the proliferation, migration, invasion and apoptosis of HGC-27 GC cells. Transfection with the Ov-TEAD4 plasmid also downregulated the expression levels of Bax and cleaved caspase-3 compared with the Ov-HOXB13 + Ov-NC group, while the upregulation of Bcl-2 was not significant (Fig. 7C and D). These results suggested

that the overexpression of TEAD4 may reverse the effects of Ov-HOXB13 on the proliferation, migration, invasion and apoptosis of HGC-27 cells.

HOXB13 inhibits the involvement of TEAD4 in the Hippo signaling pathway by regulating VGLL4 expression. To investigate the underlying mechanisms associated with the interaction between HOXB13 and TEAD4, two VGLL4 siRNAs were constructed and transfected into HGC-27 cells (Fig. 8A). As si-VGLL4-1 was found to downregulate the expression of VGLL4 to the greatest extent, it was selected for use in subsequent experiments. As shown in Fig. 8B and C, the knockdown of VGLL4 markedly upregulated TEAD4 protein and mRNA expression levels, respectively, compared with the Ov-HOXB13 + si-NC group. The JASPAR database was used to predict that HOXB13 is a potential transcription factor that can bind to the promoter of VGLL4. As exhibited in Fig. 8D, two putative binding sites (S1/S2) of HOXB13 were identified in the VGLL4 promoter. Luciferase reporter plasmid containing WT-VGLL4-S1 or WT-VGLL4-S2 sites
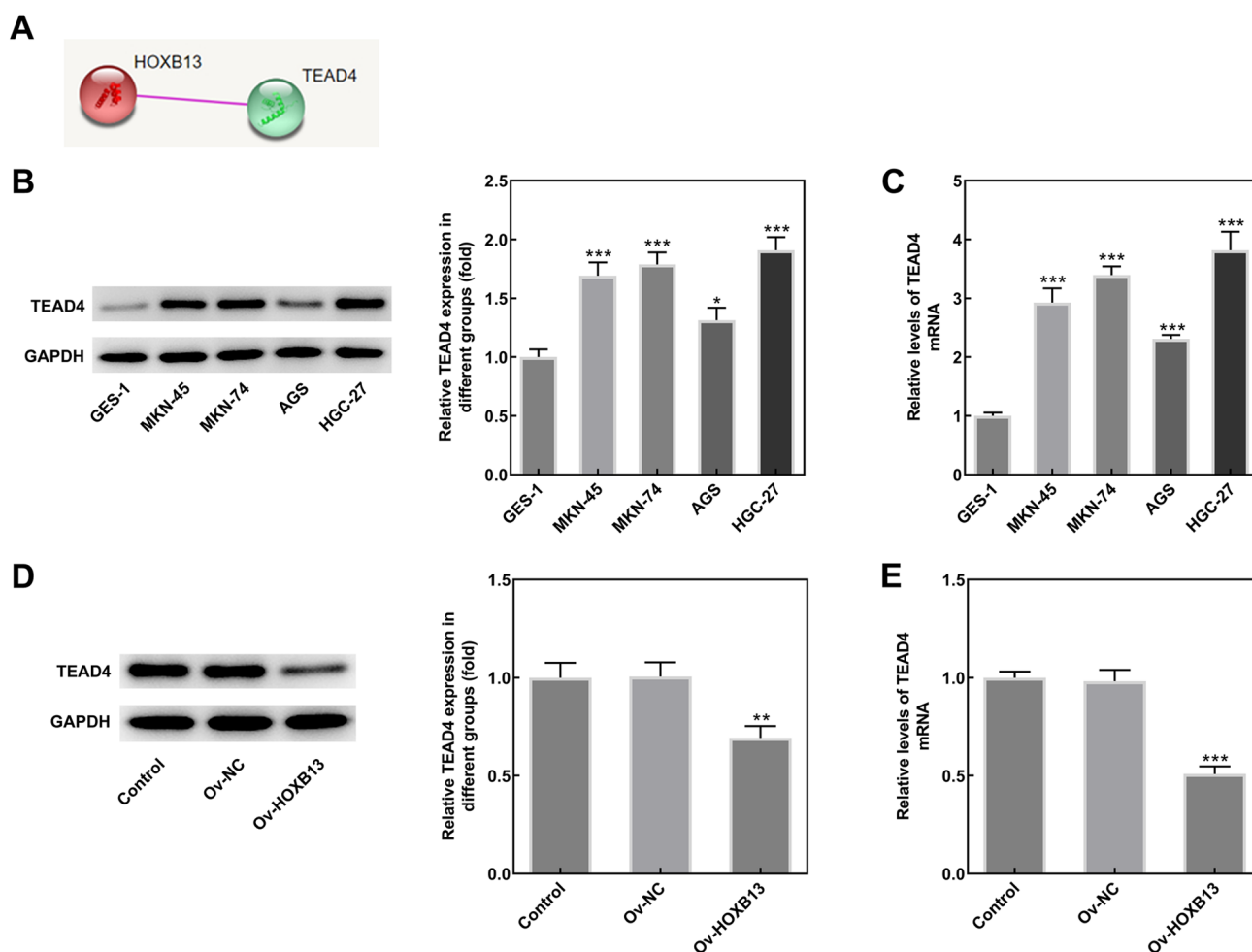
Figure 4. Overexpression of HOXB13 downregulates TEAD4 expression in HGC-27 GC cells. (A) Interaction between HOXB13 and TEAD4 was predicted using the Search Tool for the Retrieval of Interacting Genes/Proteins database. (B) TEAD4 protein and (C) mRNA expression levels in several human GC cell lines (MKN-45, MKN-74, AGS and HGC-27) and GES-1 cells were determined by western blotting and RT-qPCR, respectively. $^{*}P<0.05$, $^{***}P<0.001$ vs. GES-1. (D) TEAD4 protein and (E) mRNA expression levels in different groups (Control, Ov-NC and Ov-HOXB13) were determined by western blotting and RT-qPCR, respectively. $^{**}P<0.01$, $^{***}P<0.001$ vs. Ov-NC. GC, gastric cancer; HOXB13, homeobox B13; NC, negative control; Ov, overexpression; TEAD4, TEA domain 4; RT-qPCR, reverse transcription-quantitative PCR.

were activated following HOXB13 overexpression (Fig. 8E). Additionally, notable enrichment of VGLL4 promoter sequences (S1/S2) were obtained through ChIP using the anti-HOXB13 antibody, whereas no significant enrichment was obtained using the control IgG (Fig. 8F). Finally, the results from the western blotting analysis revealed that Ov-HOXB13 significantly downregulated the expression levels of downstream effectors of the Hippo signaling pathway, including CCN2, Cyr61 and AREG, whereas the knockdown of VGLL4 exerted the opposite effects on the expression of these proteins compared with the Ov-HOXB13 + si-NC group (Fig. 8G). These results suggested that HOXB13 may inhibit the involvement of TEAD4 in the Hippo signaling pathway by regulating VGLL4 expression.

Discussion

GC is one of the most common types of malignancy worldwide and is a leading cause of cancer-related mortality (14,15). GC is a global health burden; therefore, it is urgent to determine the potential underlying mechanisms involved in its onset and development to identify promising biomarkers for the diagnosis and treatment of GC. The results of the present study revealed that Ov-HOXB13 suppressed the proliferation, migration and invasion of HGC-27 GC cells; thus, the study subsequently investigated the underlying molecular mechanism of HOXB13 in GC.

Proliferation and metastasis are hallmarks of the malignant biological behavior of GC, and inhibiting these processes has been suggested to be crucial for improving the biomedical treatment of GC worldwide (16,17). HOXB13 was reported to act as a tumor suppressor in numerous types of human cancer, including GC (8,18). Our previous study found that HOXB13 promoted the proliferation, migration and invasion of glioblastoma by transcriptional upregulation of the long non-coding RNA (lncRNA) homeobox cluster C antisense RNA 3 (19). In the present study, HOXB13 expression was discovered to be downregulated in various cancer cell lines following analysis using the CCLE database. In addition, HOXB13 expression was downregulated in human GC cell lines compared with normal gastric cells. Moreover, the overexpression of HOXB13 inhibited the proliferation, migration and invasion of HGC-27
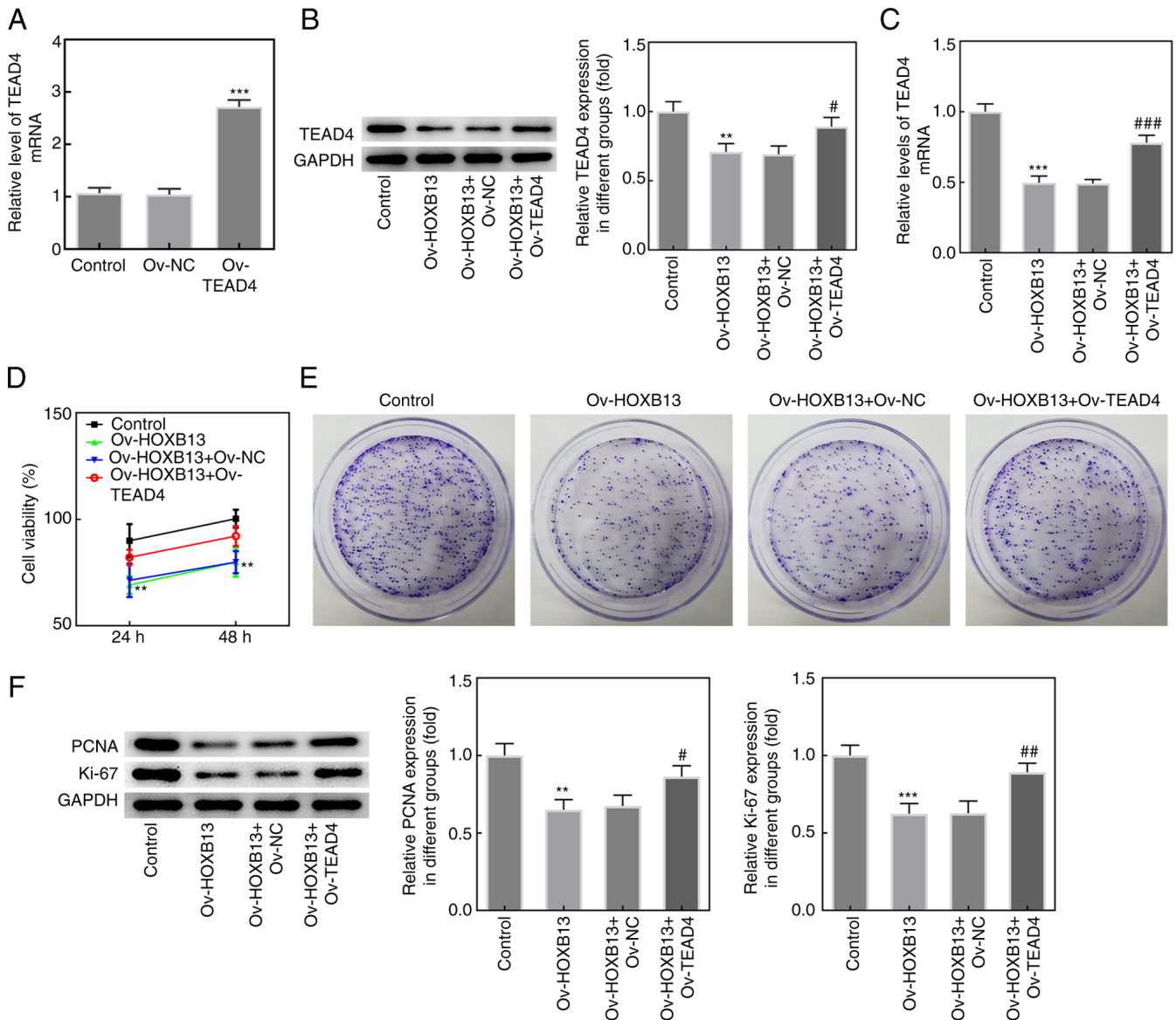
Figure 5. TEAD4 overexpression reduces the effects of HOXB13 on HGC-27 cell proliferation. (A) TEAD4 expression was evaluated with RT-qPCR after transfection with Ov-TEAD4 plasmid. ***P<0.001 vs. Ov-NC. (B) TEAD4 protein and (C) mRNA expression levels in HGC-27 cells were determined by western blotting and RT-qPCR, respectively. (D) Cell viability was detected by Cell Counting Kit-8 assay. (E) Cell proliferation was analyzed using colony formation assay. (F) The protein expression levels of PCNA and Ki-67 were determined by western blotting. **P<0.01, ***P<0.001 vs. Control; #P<0.05, ##P<0.01, ###P<0.001 vs. Ov-HOXB13 + Ov-NC. HOXB13, homeobox B13; NC, negative control; Ov, overexpression; PCNA, proliferating cell nuclear antigen; RT-qPCR, reverse transcription-quantitative PCR; TEAD4, TEA domain 4.

cells, and promoted cell apoptosis. Thus, it was suggested that HOXB13 may serve an anticarcinogenic role in GC progression. Subsequently, further experiments were performed to investigate the detailed mechanism underlying the role of HOXB13 in GC. Notably, HOXB13 was found to interact with TEAD4, as demonstrated by analysis using the STRING database. The expression levels of TEAD4 were upregulated in human GC cell lines compared with normal gastric cells. In addition, the overexpression of HOXB13 downregulated the expression levels of TEAD4 in HGC-27 cells. Lim *et al* (20) demonstrated that the expression levels of TEAD4 were upregulated in GC cells, which is consistent with the findings of the present study. Notably, Ov-TEAD4 reversed the suppressive effects of Ov-HOXB13 on the proliferation, migration and invasion, and the promoting effect on the apoptosis of HGC-27 cells in

the present study. In a previous study, TEAD4 was reported to contribute to GC progression by regulating the expression of the lncRNA motor neuron and pancreas homeobox 1 antisense RNA 1 (21). Thus, it was hypothesized that TEAD4 may mediate the effects of HOXB13 in GC progression.

Based on the discovery of genome-wide integrated expression transcriptome and immune antibody proteomics, the VGLL4 gene is on chromosome 3p25.3~3p25.2 and includes 14 exons. Wide expression of VGLL4 genes was detected in human tissues (22). VGLL4 was described as a tumor suppressor in numerous types of cancers, such as lung, breast and colorectal (23-25). A previous study has proposed that VGLL4 inhibits epithelial-mesenchymal transition in part through suppressing Wnt/β-catenin signaling pathway in gastric cancer (26). It was previously reported that VGLL4
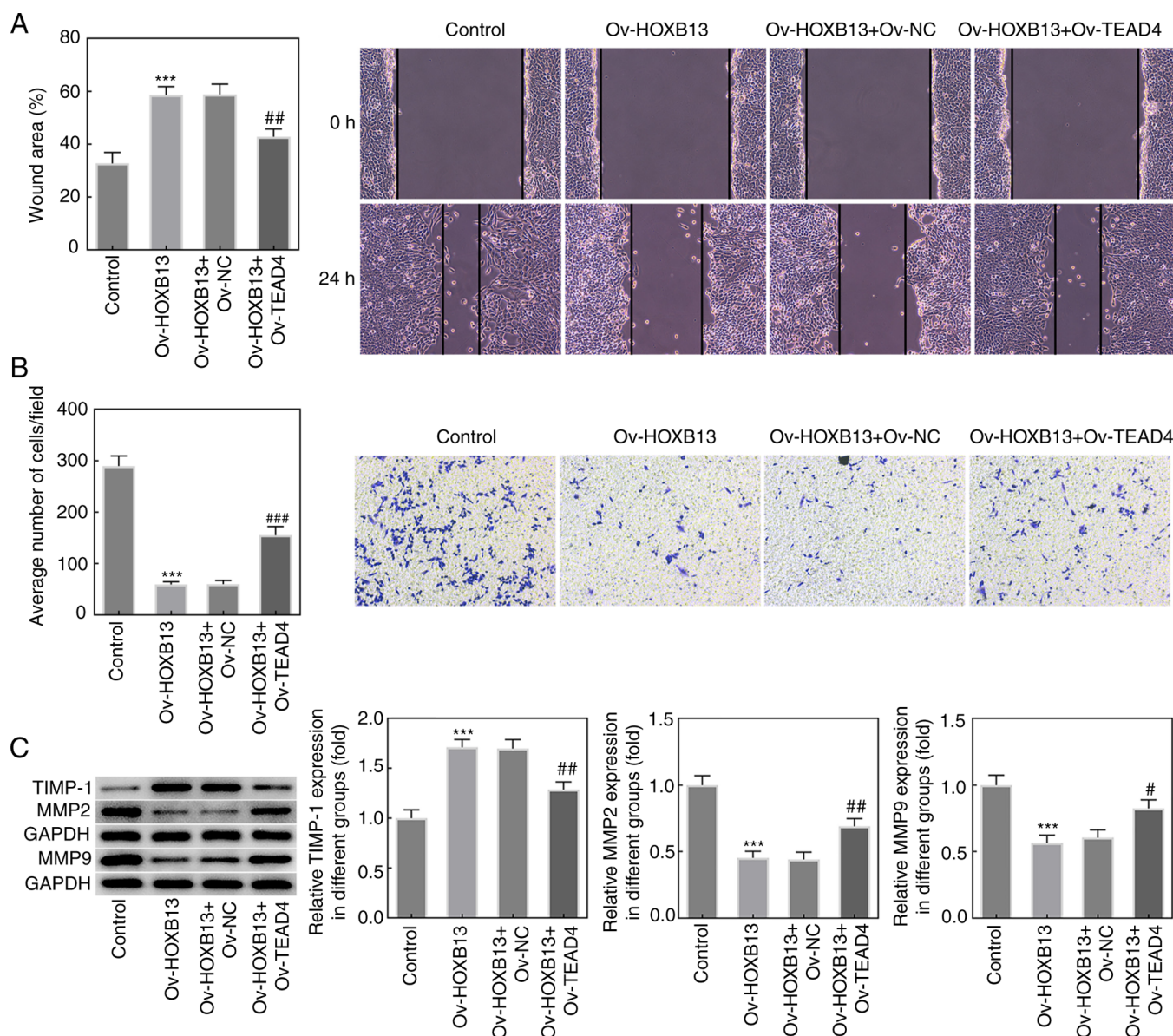
Figure 6. TEAD4 overexpression reverses the effects of HOXB13 on migration and invasion of HGC-27 cells. (A) Cell migration was examined by wound healing assay. (B) Cell invasion was analyzed by Transwell chamber assay. (C) TIMP-1, MMP2 and MMP9 protein expression levels were determined by western blotting. ***P<0.001 vs. Control; #P<0.05, ##P<0.01, ###P<0.001 vs. Ov-HOXB13 + Ov-NC. HOXB13, homeobox B13; NC, negative control; Ov, overexpression; TEAD4, TEA domain 4; TIMP, tissue inhibitor of metalloproteinases 1.

acted as a tumor suppressor in GC by directly competing with YAP for the binding to TEADs, thereby suppressing the tumor-promoting effect of the TEAD family in GC (12). The findings of the present study demonstrated that the knockdown of VGLL4 significantly upregulated TEAD4 expression levels. In addition, as a transcription factor of VGLL4, HOXB13 was found to interact with VGLL4 and upregulate its expression. Jiao et al (25) reported that VGLL4, which was previously identified as a YAP antagonist, targeted the TEAD4-transcription factor 4 complex and negatively regulated TEAD4 transactivation to inhibit colorectal carcinoma tumor growth. YAP is the effector protein of the Hippo pathway (27). As a tumor suppressor pathway, the Hippo signaling pathway is involved in multiple cellular processes driving cell proliferation and differentiation, and its dysregulation was found to contribute to the tumorigenesis of multiple cancer types (28). The results

of the present study revealed that the knockdown of VGLL4 reversed the suppressive effects of HOXB13 on the expression levels of downstream effectors of the Hippo signaling pathway, including CCN2, Cyr61 and AREG, suggesting that HOXB13 may inhibit the involvement of TEAD4 in the Hippo signaling pathway by regulating VGLL4 expression.

In conclusion, the findings of the present study suggested that HOXB13 may suppress the proliferation, migration and invasion, and promote the apoptosis of GC cells through the transcriptional activation of VGLL4 to inhibit the involvement of TEAD4 in the Hippo signaling pathway. These results may provide evidence for a new regulatory mechanism involving HOXB13 in GC, suggesting a theoretical basis for the development of novel targeted therapies. The lack of experimental verification of the direct interaction mechanism between VGLL4 and TEAD4 is a potential limitation of the present study and an
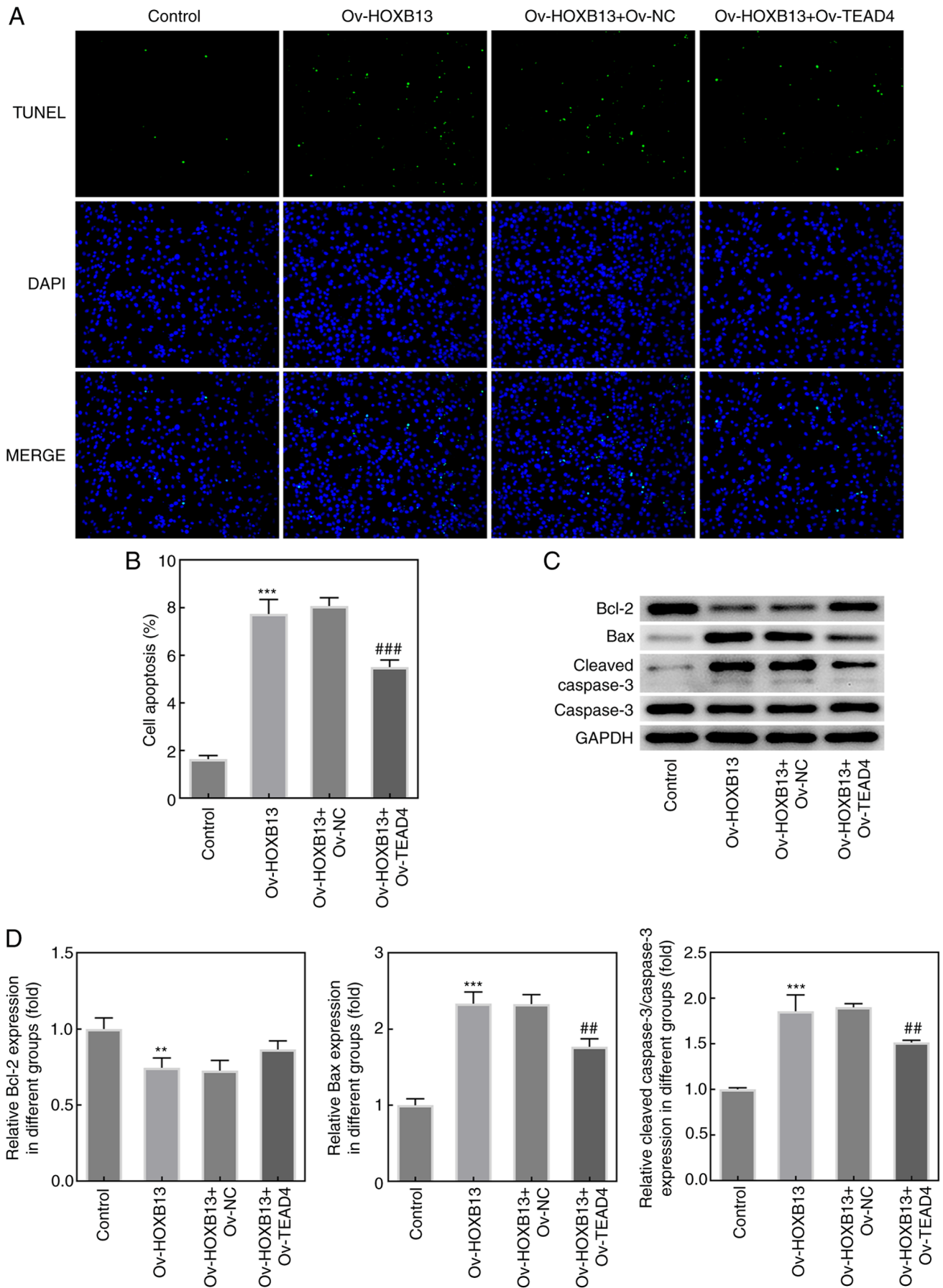
Figure 7. TEAD4 overexpression abolishes the effects of HOXB13 on apoptosis of HGC-27 cells. (A) Apoptosis was detected with TUNEL assay and (B) quantified. (C) Expression levels of apoptosis-related proteins Bcl-2, Bax and cleaved caspase3 were determined using western blot analysis and (D) semi-quantified. **P<0.01, ***P<0.001 vs. Control; ##P<0.01, ###P<0.001 vs. Ov-HOXB13 + Ov-NC. HOXB13, homeobox B13; NC, negative control; Ov, overexpression; TEAD4, TEA domain 4.
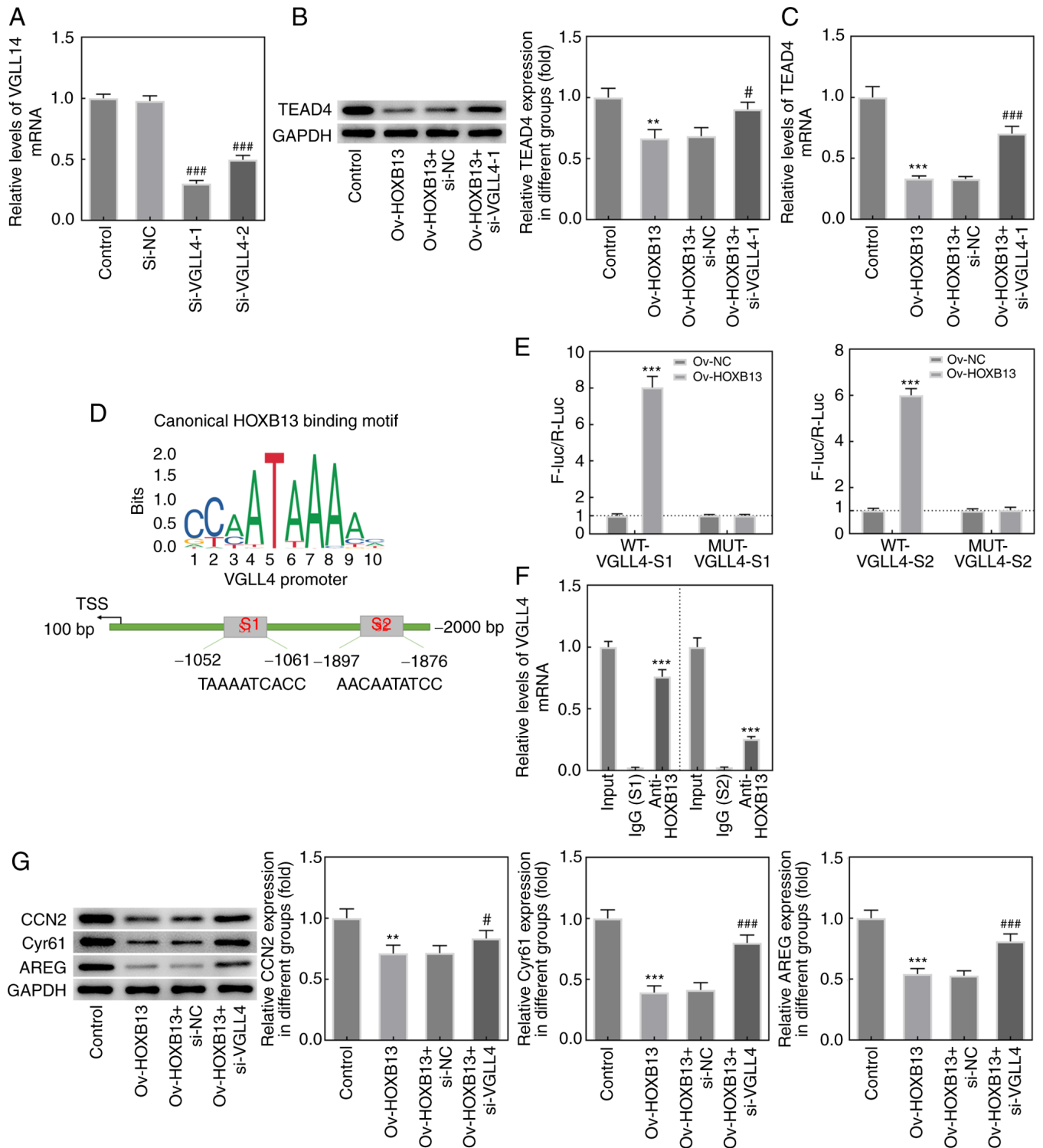
Figure 8. HOXB13 inhibits the involvement of TEAD4 in Hippo signaling pathway by regulating VGLL4 expression. (A) Relative mRNA expression levels of VGLL4 in transfected HGC-27 cells were examined by RT-qPCR. ###$P<0.001$ vs. si-NC. (B) Protein and (C) mRNA expression levels of TEAD4 in HGC-27 cells were determined by western blot assay and RT-qPCR, respectively. **$P<0.01$, ***$P<0.001$ vs. Control; #$P<0.05$, ###$P<0.001$ vs. Ov-HOXB13 + si-NC. (D) The binding of HOXB13 to VGLL4 promoter regions (S1/S2). (E) The interaction between HOXB13 and VGLL4 was determined by luciferase reporter gene assay. ***$P<0.001$ vs. Ov-NC. (F) The direct binding of HOXB13 and VGLL4 promoter was confirmed using chromatin immunoprecipitation. ***$P<0.001$ vs. IgG. (G) Protein expression levels of downstream effectors of the Hippo signaling pathway, including CCN2, Cyr61 and AREG, were determined with western blot analysis and semi-quantified. **$P<0.01$, ***$P<0.001$ vs. Control; #$P<0.05$, ###$P<0.001$ vs. Ov-HOXB13 + si-NC. AREG, amphiregulin; CCN2, cellular communication network factor 2; Cyr61, cysteine rich angiogenic inducer 61; HOXB13, homeobox B13; F-luc/R-Luc, Firefly luciferase/*Renilla* luciferase; MUT, mutant-type; NC, negative control; Ov, overexpression; si, small interfering RNA; TEAD4, TEA domain 4; TSS, transcription start site; VGLL4, vestigial-like family member 4; WT, wild-type; RT-qPCR, reverse transcription-quantitative PCR; S1, site 1; S2, site 2.

aim of future studies. Additionally, the potential use of GSEA to assess more collectively through bioinformatics analysis the

association between HOXB13 expression and Hippo signaling pathways will be also performed in future studies.

Availability of data and materials

The datasets used and/or analyzed during the current study are available from the corresponding author on reasonable request.

Authors' contributions

HG designed the study and wrote the manuscript. HG, GL, JH, JL, DW and SZ performed the experiments and analyzed the data. XX conceived and supervised the study and co-wrote the manuscript. XX and HG confirm the authenticity of all the raw data. All authors have read and approved the final manuscript.

Ethics approval and consent to participate

Not applicable.

Patient consent for publication

Not applicable.

Competing interests

The authors declare that they have no competing interests.

References

1. Smyth EC, Nilsson M, Grabsch HI, van Grieken NC and Lordick F: Gastric cancer. Lancet 396: 635-648, 2020.
2. Machlowska J, Baj J, Sitarz M, Maciejewski R and Sitarz R: Gastric cancer: Epidemiology, risk factors, classification, genomic characteristics and treatment strategies. Int J Mol Sci 21: 4012, 2020.
3. Thrift AP and El-Serag HB: Burden of gastric cancer. Clin Gastroenterol Hepatol 18: 534-542, 2020.
4. VanOpstall C, Perike S, Brechka H, Gillard M, Lamperis S, Zhu B, Brown R, Bhanvadia R and Griend DJV: MEIS-mediated suppression of human prostate cancer growth and metastasis through HOXB13-dependent regulation of proteoglycans. Elife 9: e53600, 2020.
5. Xie B, Bai B, Xu Y, Liu Y, Lv Y, Gao X, Wu F, Fang Z, Lou Y, Pan H and Han W: Tumor-suppressive function and mechanism of HOXB13 in right-sided colon cancer. Signal Transduct Target Ther 4: 51, 2019.
6. Wang X, Wang R, Wu Z and Bai P: Circular RNA ITCH suppressed prostate cancer progression by increasing HOXB13 expression via spongy miR-17-5p. Cancer Cell Int 19: 328, 2019.
7. Okuda H, Toyota M, Ishida W, Furihata M, Tsuchiya M, Kamada M, Tokino T and Shuin T: Epigenetic inactivation of the candidate tumor suppressor gene HOXB13 in human renal cell carcinoma. Oncogene 25: 1733-1742, 2006.
8. Sui BQ, Zhang CD, Liu JC, Wang L and Dai DQ: HOXB13 expression and promoter methylation as a candidate biomarker in gastric cancer. Oncol Lett 15: 8833-8840, 2018.
9. Guo C, Chu H, Gong Z, Zhang B, Li C, Chen J and Huang L: HOXB13 promotes gastric cancer cell migration and invasion via IGF-1R upregulation and subsequent activation of PI3K/AKT/mTOR signaling pathway. Life Sci 278: 119522, 2021.
10. Zhou Y, Huang T, Zhang J, Wong CC, Zhang B, Dong Y, Wu F, Tong JHM, Wu WKK, Cheng ASL, *et al*: TEAD1/4 exerts oncogenic role and is negatively regulated by miR-4269 in gastric tumorigenesis. Oncogene 36: 6518-6530, 2017.
11. Han Y: Analysis of the role of the Hippo pathway in cancer. J Transl Med 17: 116, 2019.
12. Jiao S, Wang H, Shi Z, Dong A, Zhang W, Song X, He F, Wang Y, Zhang Z, Wang W, *et al*: A peptide mimicking VGLL4 function acts as a YAP antagonist therapy against gastric cancer. Cancer Cell 25: 166-180, 2014.
13. Livak KJ and Schmittgen TD: Analysis of relative gene expression data using real-time quantitative PCR and the 2(-Delta Delta C(T)) method. Methods 25: 402-408, 2001.
14. Machlowska J, Maciejewski R and Sitarz R: The pattern of signatures in gastric cancer prognosis. Int J Mol Sci 19: 1658, 2018.
15. Van Cutsem E, Sagaert X, Topal B, Haustermans K and Prenen H: Gastric cancer. Lancet 388: 2654-2664, 2016.
16. Yang Q, Tian S, Liu ZR and Dong WG: Knockdown of RIPK2 inhibits proliferation and migration, and induces apoptosis via the NF-k B signaling pathway in gastric cancer. Front Genet 12: 627464, 2021.
17. Zeng MM, Li BX, Yang L and Guan QL: CBX2 depletion inhibits the proliferation, invasion and migration of gastric cancer cells by inactivating the YAP/β-catenin pathway. Mol Med Rep 23: 137, 2021.
18. Cannon-Albright LA, Stevens J, Teerlink CC and Agarwal N: The HOXB13 p.Gly84Glu variant observed in an extended five generation high-risk prostate cancer pedigree supports risk association for multiple cancer sites. Cancer Epidemiol 69: 101834, 2020.
19. Wang X, Sun Y, Xu TY, Qian K, Huang B, Zhang K, Song Z, Qian T, Shi J and Li L: HOXB13 promotes proliferation, migration, and invasion of glioblastoma through transcriptional upregulation of lncRNA HOXC-AS3. J Cell Biochem 120: 15527-15537, 2019.
20. Lim B, Kim HJ, Heo H, Huh N, Baek SJ, Kim JH, Bae DH, Seo EH, Lee SI, Song KS, *et al*: Epigenetic silencing of miR-1271 enhances MEK1 and TEAD4 expression in gastric cancer. Cancer Med 7: 3411-3424, 2018.
21. Shuai Y, Ma Z, Liu W, Yu T, Yan C, Jiang H, Tian S, Xu T and Shu Y: TEAD4 modulated LncRNA MNX1-AS1 contributes to gastric cancer progression partly through suppressing BTG2 and activating BCL2. Mol Cancer 19: 6, 2020.
22. Fagerberg L, Hallstrom BM, Oksvold P, Kampf C, Djureinovic D, Odeberg J, Habuka M, Tahmasebpoor S, Danielsson A, Edlund K, *et al*: Analysis of the human tissue-specific expression by genome-wide integration of transcriptomics and antibody-based proteomics. Mol Cell Proteomics 13: 397-406, 2014.
23. Zhang WJ, Gao YJ, Li PX, Shi Z, Guo T, Li F, Han X, Feng Y, Zheng C, Wang Z, *et al*: VGLL4 functions as a new tumor suppressor in lung cancer by negatively regulating the YAP-TEAD transcriptional complex. Cell Res 24: 331-343, 2014.
24. Zhang Y, Shen H, Withers H, Yang N, Denson KE, Mussell AL, Truskinovsky A, Fan Q, Gelman IH, Frangou C and Zhang J: VGLL4 selectively represses YAP-dependent gene induction and tumorigenic phenotypes in breast cancer. Sci Rep 7: 6190, 2017.
25. Jiao S, Li C, Hao Q, Miao H, Zhang L, Li L and Zhou Z: VGLL4 targets a TCF4-TEAD4 complex to coregulate Wnt and Hippo signalling in colorectal cancer. Nat Commun 8: 14058, 2017.
26. Li H, Wang Z, Zhang W, Qian K, Liao G, Xu W and Zhang S: VGLL4 inhibits EMT in part through suppressing Wnt/β-catenin signaling pathway in gastric cancer. Med Oncol 32: 83, 2015.
27. Sugihara T, Isomoto H, Gores G and Smoot R: YAP and the Hippo pathway in cholangiocarcinoma. J Gastroenterol 54: 485-491, 2019.
28. Stanger BZ: Quit your YAPing: A new target for cancer therapy. Genes Dev 26: 1263-1267, 2012.